ELSEVIER

Journal of Magnetism and Magnetic Materials 249 (2002) 220–227

journal of magnetism and magnetic materials

www.elsevier.com/locate/jmmm

Preparation and magnetic behavior of arrays of electrodeposited Co nanowires

J. Rivas[a,*], A. Kazadi Mukenga Bantu[a,1], G. Zaragoza[b], M.C. Blanco[b], M.A. López-Quintela[b]

[a] *Applied Physics Department, University of Santiago de Compostela, E-15782 Santiago de Compostela, Spain*
[b] *Physical Chemistry Department, University of Santiago de Compostela, E-15782 Santiago de Compostela, Spain*

Abstract

Cobalt nanowires have been synthesized by electrodeposition into porous track-etched polycarbonate membranes with a quoted pore diameter of $D_p \approx 200-400$ nm and a thickness of $L \approx 7$ μm. Magnetization curves and torque experiments of arrays of Co wires confirm that when the lengths of the wires are increased a crossover takes place from a parallel easy direction of magnetization towards an easy direction perpendicular to the axis of the wire. This change in the easy direction of magnetization is analyzed considering the competition between demagnetizing field, magnetocrystalline anisotropy, and dipolar interaction among wires.

PACS: 75.30.Gw; 75.50.−y; 75.60.−d

Keywords: Arrays of Co nanowires; Magnetocrystalline anisotropy; Magnetic dipolar interactions

1. Introduction

Nanometer-scale magnets are of great interest for magnetic storage and novel electronic devices [1]. Most magnetic devices such as storage devices, spin valves or magnetic sensors used today are based on nanometer-scale magnetic elements. Nanofabrication technology offers unprecedented capabilities in manufacturing materials with a size smaller than the magnetic domain wall, and in manipulating the size, shape and orientation of the structure [2]. The behavior of nanoscale magnetic structures is exotic and allows them to reach the limits of the fundamentals of micromagnetism [3].

There are several methods to fabricate large arrays of magnetic materials [4a–c], for instance by lithography, e-beam lithography, etc., but electrodeposition of metals into the pores of polymeric membranes [5,6] or anodic porous alumina [7,8] is the most inexpensive technique to produce large-scale periodic nanostructures of magnetic materials.

In this paper we use a simple electrochemical route for the preparation of arrays of Co wires up to a length $L \leqslant 7$ μm in track-etched polycarbonate membranes. The magnetic properties of these

*Corresponding author. Tel.: 34-981-563100x14021; fax: 34-981-520676.

E-mail address: farivas@uscmail.usc.es (J. Rivas).

[1] Also at Physics Department, Faculty of Sciences, University of Kinshasa, P.O. Box 190 Kinshasa 11, Democratic Republic of the Congo (Zaïre).

0304-8853/02/$ - see front matter
PII: S0304-8853(02)00534-6

arrays of electrodeposited Co wires show a magnetization reversal that appears to depend on wire length. These magnetic results are interpreted taking into account the demagnetizing field, magnetocrystalline anisotropy, and magnetic dipolar coupling among wires.

2. Fabrication and structural characterization

The arrays of nanowires were obtained by electrodeposition of Co inside the pores of commercial track-etched polycarbonate membranes (Millipore–Isopore® Membrane Filters) using a silver sputtering as substrate. The polycarbonate membranes used in this work have a thickness $L \approx 7\,\mu m$, pore diameters $D_p \approx 200$ and 400 nm, and an average separation $d \approx 480$ and 830 nm between pores, respectively. The growth of nanowires was performed by electrodeposition at room temperature from a sulfate bath containing [9a] Co^{+2} ions under potentiostatic control using a conventional three-electrode cell. X-ray diffraction shows that the material deposited is essentially polycrystalline cobalt with a hexagonal close packed (HCP) structure and the hexagonal c-axis lies preferentially perpendicular to the long axis of the wires [9b]. This texture is typical for these wire diameters [10a–e], as opposed to shorter diameters (near 35 nm) which have an HCP structure with the crystalline c-axis parallel to the wire axis [3]. In any case, the final texture of the wires obviously depends on the plating procedure. In fact, Paulus et al. [10d] found that the direction of the hexagonal c-axis is nearly independent of wire diameter and that the change of the easy axis is due to an increasing amount of FCC-Co in smaller pores, whereas Fert et al. [10e] argue that this is due to a reorientation of the hexagonal c-axis.

3. Results and discussion

3.1. Magnetization measurements

A Vibrating Sample Magnetometer Digital Measurement Systems model 1660 was used to measure the hysteresis loops of samples at room temperature at maximum fields applied of $H = 11$ kOe. The measurements were made with the magnetic fields applied perpendicular or parallel to the axes of the nanowires. The normalized hysteresis loops of arrays of 200–400 nm diameter Co wires are shown in Fig. 1. Here, Fig. 1(a, c) and (b, d) correspond to short ($L < 1\,\mu m$) and long wires, respectively. It can be seen that for short wires the direction parallel to the axis of the wire is that of easy direction of magnetization, whilst as the wires increase in length the hysteresis loops tend to overlap, and this implies a change in the easy direction of magnetization.

To understand the present results a magnetostatic model was formulated taking into account the demagnetizing field, magnetocrystalline anisotropy, and dipolar interactions in the arrays of wires. For the sake of simplicity we assume that the experimental membrane is a two-dimensional array of parallel Co wires as indicated in Fig. 2. If the array is formed by a squared lattice of magnetostatic dipoles with a lattice spacing d, and the magnetization M lies along the wire axis, the total effective magnetic field, which acts on each wire, is parallel to the axis of the wire and may be expressed as

$$H_{\text{eff}\parallel} = H_{\text{dipolar}} + H_A, \tag{1}$$

where $H_{\text{dipolar}} \approx 4.2(MV/d^3)$ (where V is the volume of each wire) corresponds to the magnetostatic dipolar interactions among nanowires [11], while $H_A = (2k/M)$ is the anisotropy field associated to the uniaxial magnetocrystalline anisotropy constant k of Co. On the other hand, for the same array with the magnetization aligned perpendicular to the axes of the wires, the total effective field may be expressed as

$$H_{\text{eff}\perp} = -\tfrac{1}{2} H_{\text{dipolar}} + H_{\text{shape}}, \tag{2}$$

where H_{shape} is the demagnetizing field of each wire ($H_{\text{shape}} = 2\pi M$). In expressions (1) and (2) the positive sign corresponds to effective fields of directions opposite to the magnetization vectors. In this way, for a particular membrane, with a fixed distribution of pores, a crossover of the easy direction of magnetization is expected, when $H_{\text{eff}\parallel} = H_{\text{eff}\perp}$. For bulk Co HCP at room

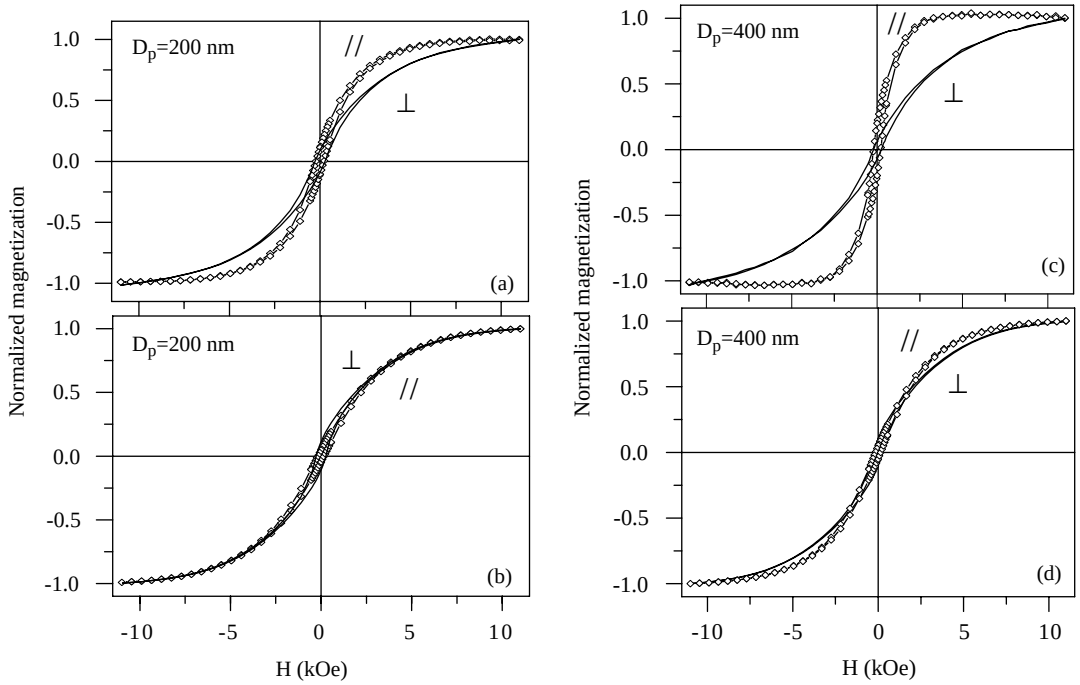

Fig. 1. Normalized hysteresis loops at room temperature of arrays of Co nanowires of (a, b) 200 and (c, d) 400 nm—diameters as a function of wire lengths, recorded with the field applied parallel (– ◇ –) and perpendicular (—) to the wire axis for (a, c) short wires and (b, d) long wires.

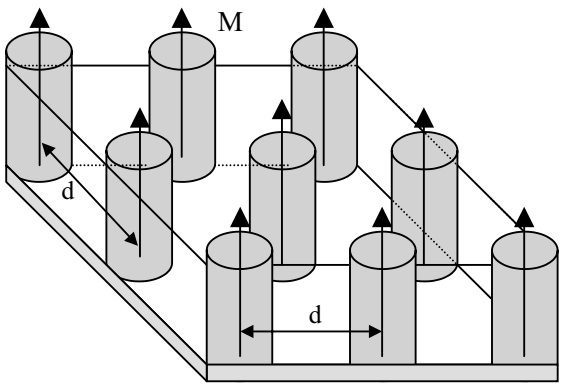

Fig. 2. Square dipolar arrays of Co wires with a lattice spacing d, when the magnetization is parallel to the wire axis.

temperature [12] the magnetocrystalline anisotropy constant is in the order of $k = 5 \times 10^6\,\mathrm{erg/cm^3}$ and $M = 1422\,\mathrm{emu/cm^3}$. In the case of the critical effective field the crossover in magnetization direction occurs when

$$\left(\frac{V}{d^3}\right)_{\text{critical}} \approx 0.21. \tag{3}$$

For values lower than 0.21 the magnetization has an easy axis parallel to the axes of the wires. For values higher than 0.21 the magnetization is perpendicular to the axes of the wires. In this way we may explain the experimental results obtained, and so for example, for an array of wires with a diameter of 400 nm and an average distance between the wires of $d \approx 830$ nm a cross-over in the direction of magnetization is expected for wires of $L \approx 1$ μm length as has been observed experimentally (see Fig. 1(d)).

3.2. Magnetic interactions

The use of remanent curves as a tool to analyze the type and strength of interaction between particles in magnetic single-domain particle

systems is widespread. It is commonly accepted that noninteracting systems in general show linear relations in the plots of the DC demagnetization remanent versus isothermal remanent curves [13–16a–c].

In Fig. 3 we show the normalized δm plots derived from DC demagnetization remanent $m_d(H) = (M_d(H)/M_r(\infty))$ and isothermal remanent $m_r(H) = (M_r(H)/M_r(\infty))$ curves for arrays of Co wires with diameters of 200 and 400 nm and various wire lengths. In the nanowire systems studied here the normalized δm plots always show a negative peak for all the samples investigated. This reveals that the predominant interaction in our samples is magnetostatic. From the experimental results one can observe that as the magnitude of magnetic interactions decreases, the lengths of the wires increase. This can be understood if we bear in mind that a crossover of the easy axis of magnetization from the parallel to perpendicular direction to the wire has occurred for the longest wires. On the other hand, the values of δm for wires with diameters of 400 nm present negative δm deviation, higher than those for wires with diameters of 200 nm. This indicates a stronger magnetic interaction among the wires with greater magnetic moment.

3.3. Torque measurements

Magnetic torque measurements at room temperature were carried out with a Torque Magnetometer Digital Measurement Systems model 1660 as a function of the length of the nanowires with diameters of 200–400 nm (see Fig. 4(a–f)). The torque intensity due to the externally applied magnetic field was measured when the normal of membrane plane was rotated with respect to the maximum applied field of 11 kOe. In order to simplify the analysis of the torque measurements we have assumed that the magnetization and applied field are nearly collinear in all cases and the fourth order anisotropy constant is negligible. In this case the θ-dependent part of the uniaxial anisotropy energy is given by

$$E = k_{\mathrm{eff}} \sin^2(\theta) \quad (\mathrm{erg/cm^3}), \tag{4}$$

where θ is the angle between magnetization and the easy direction, and the effective anisotropy constant k_{eff} can be used to quantify the crossover from a parallel easy direction of magnetization towards an easy direction perpendicular to the wires. A change from parallel ($k_{\mathrm{eff}} > 0$) to perpendicular ($k_{\mathrm{eff}} < 0$) easy magnetization axis occurs when the wire length increases. For positive k_{eff} the $\theta = 0^\circ$ and 180° positions are energy minima, and $\theta = 90^\circ$, which is a hard direction of magnetization, is a position of instability. The slope of the torque intensity curves is negative for the positions of stability ($\theta = 0^\circ$ and 180°) and positive for unstable position ($\theta = 90^\circ$) [17]. Fig. 4 shows the torque intensity curves of arrays of Co wires with diameters of 200 and 400 nm. According to the model formulated in Section 3.1 the effective constant of anisotropy could follow a linear relationship with respect to the ratio (V/d^3). Taking into account Eqs. (1) and (2) the effective anisotropy constant can be expressed as

$$k_{\mathrm{eff}} = -3.15M^2\left(\frac{V}{d^3}\right) + \pi M^2 - k \quad (\mathrm{erg/cm^3}). \tag{5}$$

Fig. 5 shows the effective anisotropy constant k_{eff} as a function of (V/d^3), measured (from Fig. 4) and calculated from Eq. (5) taking into account the values of M and k of Co previously given. One can see that for both wire diameters (200 and 400 nm) the k_{eff} experimental values reproduce the tendency of Eq. (5), i.e. a decrease in k_{eff} appears as (V/d^3) increases. The samples with diameters of 400 nm are those, which correspond most closely to the theoretical model (broken line) because, as we have seen in the previous section, the magnetostatic interaction is greater in the samples with diameters of 200 nm.

The greatest deviations of experimental results with regard to expression (5), in the wires with smaller diameter (200 nm) may be partially attributable to the dipole–dipole interaction, unlike those of the model proposed. If we take this into account, we can redefine Eq. (5) as

$$k_{\mathrm{eff}} = -3.15\alpha M^2\left(\frac{V}{d^3}\right) + \pi M^2 - k \quad (\mathrm{erg/cm^3}), \tag{6}$$

where α is a weight factor ($0 \leqslant \alpha \leqslant 1$) which measures the importance of the magnetostatic

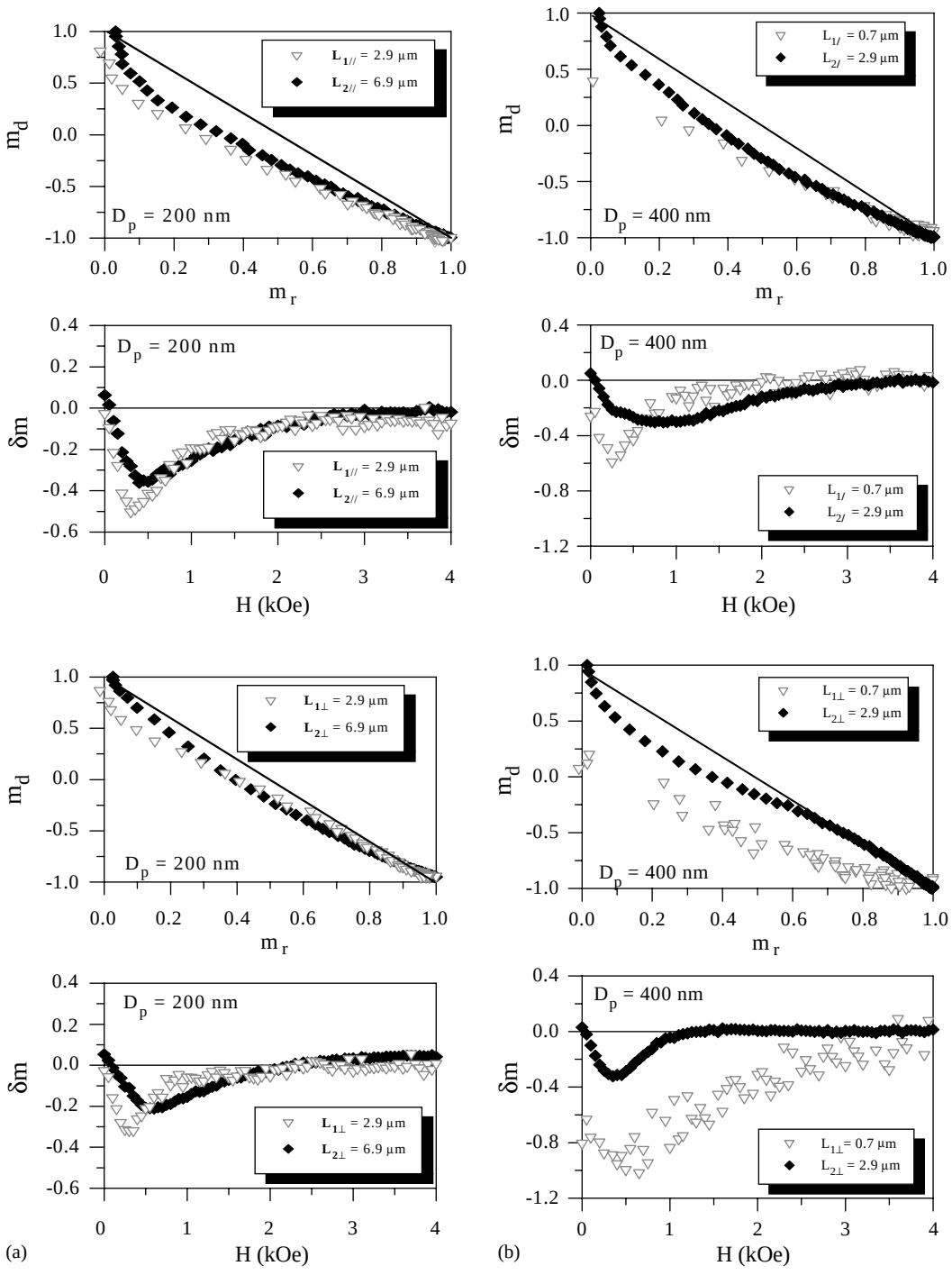

Fig. 3. Normalized remanent curves and δm plots for Co wires of (a) 200 and (b) 400 nm in diameter with the applied field perpendicular and parallel to the wire axis for short (▽) and long wires (◆).

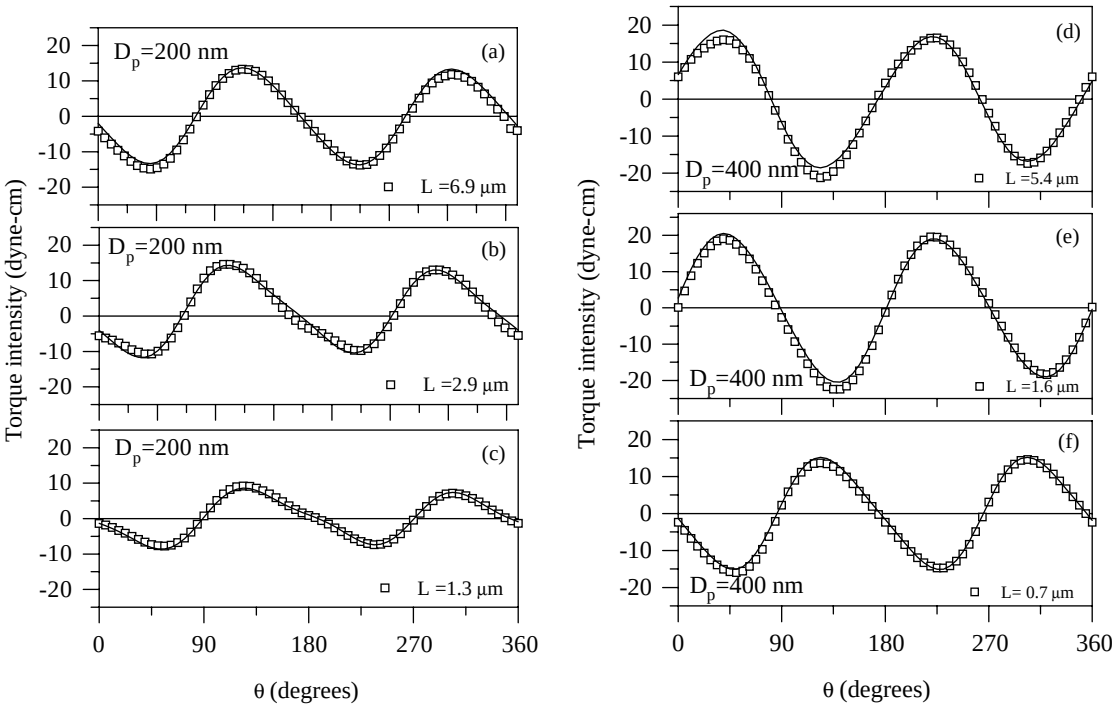

Fig. 4. Measured (□) and calculated (——) torque intensity curves at room temperature of a series of arrays of Co wires with (a–c) 200 and (d–f) 400 nm diameters as functions of wire lengths, with (a) $L = 6.9\,\mu m$, (b) $L = 2.9\,\mu m$, (c) $L = 1.3\,\mu m$ and, (d) $L = 5.4\,\mu m$, (e) $L = 1.6\,\mu m$ and (f) $L = 0.7\,\mu m$, respectively.

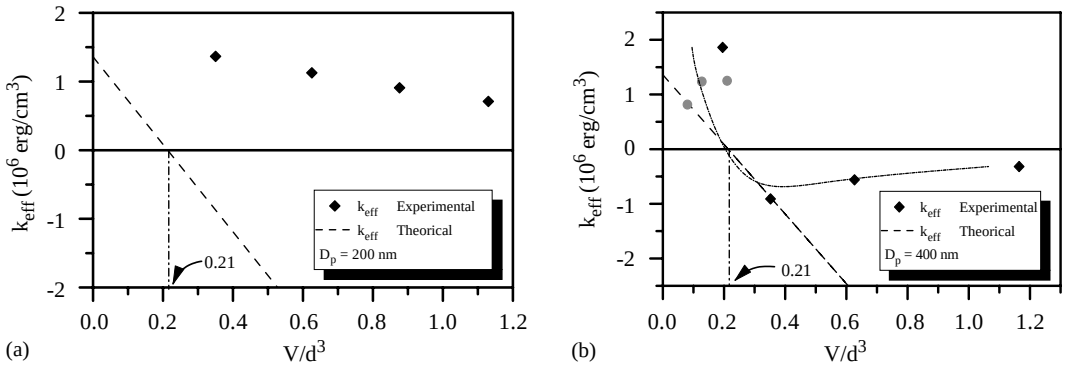

Fig. 5. Dependence of the effective anisotropy constant, k_{eff}, of Co wire arrays for (a) 200 and (b) 400 nm—diameters as a function of the ratio V/d^3, where V is the volume of wire and d the average distance between wires. k_{eff} measured (◆) and calculated (– – –) from torque measurements and Eq. (5), respectively. The solid circle (●) data are data measured with preparation conditions different from those of the solid diamonds (◆).

dipolar coupling. Thus, when this factor tends to zero, the effective constant of anisotropy tends to have a constant value of $k_{eff} \approx \pi M^2 - k \approx 1.35 \times 10^6\,erg/cm^3$. Moreover, as the length of the nanowire increases above the $(V/d^3)_{critical} \approx 0.21$ value, the preferential orientation of the easy direction of magnetization changes from parallel to perpendicular to the wire axis. This is shown

with the sign change of the effective anisotropy constant for wires with diameter of 400 nm. Strijkers et al. [7] and Schwanbeck et al. [18] have observed this in electrodeposited Co wires in polycarbonate membranes too. Thus, fitting the wire lengths and the average distance between them, one could control the competition between the dipolar interaction and demagnetizing field in order to have a perpendicular or parallel easy direction of magnetization. Finally, we would like to mention that the presence of asymmetrical sine curves in torque measurements is probably due to the fact that the hypothesis of collinearity between the direction of magnetization and the maximum applied field of $H_{\max} = 11\,\text{kOe}$ is not totally correct. This may be confirmed by the fact that the maximum applied field is not large enough to saturate the hysteresis loops of the arrays of Co wires, as they increase in length (see Fig. 1).

4. Conclusions

In summary, Co nanowires with diameters of 200 and 400 nm have been successfully synthesized by electrodeposition into commercial track-etched polycarbonate membranes with a thickness of $L \approx 7\,\mu\text{m}$. It has been observed that the magnetic properties depend on the wire diameters, lengths and separations between them. Thus, one can notice that the easy direction of magnetization changes when the lengths of wires vary. In the cases of the shortest wires ($L < 1\,\mu\text{m}$) the easy direction of magnetization is parallel to the axes of the wires and in the cases of the longest wires it tends to be more perpendicular. Remanent curve measurements clearly indicate that the predominant interactions among wires are of the magnetostatic type. For torque magnetic measurements it is found that the sign of the effective anisotropy constant is gradually changed when the lengths of Co wires vary. In the case of shortest wires with diameter 400 nm $k_{\text{eff}} > 0$ and for the longest wires $k_{\text{eff}} < 0$, concur with the inversion of magnetization from the direction preferential parallel to one perpendicular to the axes of wires. A simple model has been proposed which explains the results taking into account the competition between the demagnetizing fields, magnetocrystalline anisotropy of Co, and dipole–dipole interactions. This model predicts an inversion of magnetization for critical values around $(V/d^3) \approx 0.21$.

Acknowledgements

A. Kazadi would like to thank the AECI (Spanish Agency for International Cooperation) for financing his Ph.D. Thesis.

References

[1] L. Kong, S.Y. Chou, J. Appl. Phys. 80 (1996) 5205 and references therein.
[2] S.Y. Chou, IEEE Proc. 85 (4) (1997) 652.
[3] R. Ferré, K. Ounadjela, J.M. George, L. Piraux, S. Dubois, Phys. Rev. B 56 (1997) 14066.
[4] (a) T.M. Withney, et al., Science 261 (1995) 1466.
(b) G.A. Niklasson, Nanostruct. Mater. 12 (1999) 725.
(c) Y. Li, et al., Appl. Phys. Lett. 76 (2000) 2011.
[5] B. Voegeli, A. Blondel, B. Doudin, Jh.-Ansermet, J. Magn. Magn. Mater. 151 (1995) 388.
[6] T. Thurn-Albrecht, J. Schotter, G.A. Kästle, N. Emley, T. Shibanchi, L. Krusin-Elbaum, K. Guarini, C.T. Black, M.T. Tuominen, T.P. Russell, Science 290 (2000) 2126.
[7] G.J. Strijkers, J.H.J. Dalderop, M.A.A. Broeksteeg, H.J.M. Swagten, W.J.M. de Jonge, J. Appl. Phys. 86 (9) (1999) 5141.
[8] J.M. García, A. Asenjo, J. Velázquez, D. García, M. Vázquez, P. Aranda, E. Ruiz-Hitzky, J. Appl. Phys. 85 (8) (1999) 5480.
[9] (a) A. Kazadi Mukenga Bantu, J. Rivas, G. Zaragoza, M.A. López-Quintela, M.C. Blanco, J. Non-Cryst. Solids 287 (2001) 5.
(b) A. Kazadi Mukenga Bantu, J. Rivas, G. Zaragoza, M.A. López-Quintela, M.C. Blanco, J. Appl. Phys. 89 (6) (2001) 3393 and references therein.
[10] (a) J.-L. Maurice, D. Imhoff, P. Etienne, O. Durant, S. Dubois, L. Piraux, J.-M. George, P. Galtier, A. Fert, J. Magn. Magn. Mater. 184 (1998) 1.
(b) L. Piraux, S. Dubois, J.L. Duvail, K. Ounadjela, A. Fert, J. Magn. Magn. Mater. 175 (1997) 127.
(c) L. Piraux, S. Dubois, E. Ferain, R. Legras, K. Ounadjela, J.-M. George, J.-L. Maurice, A. Fert, J. Magn. Magn. Mater. 165 (1997) 352.
(d) P.M. Paulus, F. Luis, M. Kröll, G. Schimd, L.J. De Jongh, J. Magn. Magn. Mater. 224 (2001) 180.
(e) A. Fert, L. Piraux, J. Magn. Magn. Mater. 200 (1999) 338.
[11] M. Grimsditch, Y. Jaccard, I.K. Schuller, Phys. Rev. B 58 (17) (1998) 11539.

[12] R.M. Bozorth, Ferromagnetism, IEEE Press, New York, 1994, p. 867.
[13] E.P. Wohlfath, J. Appl. Phys. 29 (1958) 595.
[14] O. Henkel, Phys. Stat. Sol. 7 (1964) 919.
[15] P.E. Kelly, K. O'Grady, P.I. Mayo, R.W. Chantrell, IEEE Trans. Magn. 25 (1989) 3881.
[16] (a) M. El-Hilo, K. O'Grady, P.I. Mayo, R.W. Chantrell, I.L. Sanders, J.K. Howard, IEEE Trans. Magn. 28 (1992) 3282.
(b) P.I. Mayo, A. Brandbury, R.W. Chantrell, P.E. Kelly, H.E. Jones, P.R. Bissel, IEEE Trans. Magn. 26 (1990) 228.
(c) G.P. Heydon, S.R. Farley, S.L. Tomlinson, M.S. Valera, K. Attenborough, W. Schwarzacher, J. Phys. D: Appl. Phys. 30 (1997) 1083.
[17] B.D. Cullity, Introduction to Magnetic Materials, Addison-Wesley, Massachusetts, 1972, p. 216.
[18] H. Schwanbeck, U. Schmidt, Electrochim. Acta 45 (27) (2000) 4389.